



Alternative splicing variants involved in pyroptosis and cuproptosis contribute to phenotypic remodeling of the tumor microenvironment in cervical cancer

Kewei Bi¹ · Jialin Yang² · Xuge Wei³

Received: 5 February 2023 / Accepted: 4 June 2023

© The Author(s), under exclusive licence to Society for Reproductive Investigation 2023

Abstract

Cervical cancer (CC) remains a prevalent gynecological malignancy, posing a significant health burden among women worldwide. With the remarkable discoveries of cellular pyroptosis and cuproptosis, there has been a growing focus on exploring the intricate relationship between these two forms of cell death and their impact on tumor progression. In recent years, alternative splicing has emerged as a significant field in cancer research. Thus, the integration of alternative splicing, pyroptosis, and cuproptosis holds immense value in studying their collective impact on the occurrence and progression of cervical cancer. In this study, alternative splicing data of pyroptosis- and cuproptosis-associated genes were integrated with public databases, including TCGA, to establish a prognostic model for cervical cancer based on COX regression modeling. Subsequently, the tumor microenvironment (TME) phenotypes in the high-risk and low-risk patient groups were characterized through a comprehensive bioinformatics analysis. The findings of this study revealed that the low-risk group exhibited a predominant immune-active TME phenotype, while the high-risk group displayed a tumor-favoring metabolic phenotype. These results indicate that the alternative splicing of pyroptosis- and cuproptosis-associated genes plays a pivotal role in remodeling the phenotypic landscape of the cervical cancer TME by modulating immune responses and metabolic pathways. This study provides valuable insights into the interplay between alternative splicing variants involved in pyroptosis and cuproptosis and the TME, contributing to a deeper understanding of cervical cancer pathogenesis and potential therapeutic avenues.

Keywords Cervical cancer · Phenotype remodeling of tumor microenvironment · Alternative splicing · Pyroptosis · Cuproptosis · TCGA · Immune evasion

Introduction

Cervical cancer (CC) is one of the most common female malignancies, continuing to be a significant health burden for women, responsible for nearly 8% of all female cancer-related mortality globally [1, 2]. Despite advancements in the understanding of CC pathogenesis, the intricate

molecular mechanisms underlying this disease remain incompletely elucidated. While human papillomavirus (HPV) is the primary etiological factor for cervical cancer (CC), it is noteworthy that approximately 5% of cases are unrelated to HPV infection, indicating the complexity of the phenotype, particularly the immune phenotype, in CC [1].

As the advancing of biomedicine, multiple newfound cell death modalities have been discovered and become the spotlights in cancer immunotherapy including pyroptosis and cuproptosis [3-7]. Pyroptosis is an inflammatory form of regulated cell death characterized by the activation of inflammatory caspases and the subsequent release of pro-inflammatory cytokines. It plays a critical role in host defense against microbial infections and is also implicated in cancer development. Recent studies have demonstrated dysregulation of pyroptosis-related genes and proteins was associated with CC [8-12]. However, with respect to the roles of pyroptosis playing during the tumorigenesis and progression

✉ Xuge Wei
weixuge@symc.edu.cn

¹ Department of Physiology, College of Basic Medicine, Shenyang Medical College, Shenyang, China

² Department of Pathology, College of Basic Medicine, Shenyang Medical College, Shenyang, China

³ Department of Bioinformatics, Faculty of Biology, College of Basic Medicine, Shenyang Medical College, Shenyang, China

of tumors, it seems to be a bit of intricate because sometimes, it showed an entirely opposite effect.

On one hand, pyroptosis acts as an inflammatory cell death mechanism that restricts tumor progression. On the other hand, tumors can hijack pyroptosis to orchestrate the release of inflammatory factors, thereby promoting their own overgrowth [13]. Cuproptosis, another form of cell death, is induced by cellular copper overload and subsequent copper-induced toxicity. Copper homeostasis is tightly regulated by various transporters and chaperones, and disturbances in this equilibrium have been associated with CC [14, 15]. Similar to pyroptosis, the influence of cuproptosis on tumors also remains enigmatic, coexisting of tumor-inhibited and -promoting roles [16]. As an essential metallic element to cellular metabolism, copper is a double-edged sword, the dysregulation of which results in serious diseases, CC included [17, 18]. Since the discovery of cuproptosis, emerging studies unveiled the correlation between cuproptosis-related factors and clinical patients' prognosis of tumors [19–22]. It is reported that intratumoral copper facilitates PD-L1-driven tumor immune evasion, implying the correlation between copper-death-related participants and immune elusion [23].

Alternative splicing (AS) is a distinctive process that occurs in eukaryotes and is prevalent in the majority of genes. It provides a mechanism for generating multiple transcript variants from a single gene, thereby expanding the functional diversity of the gene [24, 25]. Alternative splicing events affecting these genes may influence the regulation of pyroptosis and cuproptosis, which contribute to CC progression. The relationship between gene alternative splicing and cell death processes, including pyroptosis and cuproptosis, in CC is an emerging area of research. Several studies have highlighted the impact of alternative splicing events on the expression and function of key genes involved in these cell death pathways. For example, alternative splicing isoforms of GSDMD have been identified, exhibiting distinct effects on pyroptosis induction [26]. Similarly, alternative splicing events affecting copper transporters can alter their cellular localization or activity, ultimately influencing cuproptosis susceptibility [27]. In conclusion, gene alternative splicing plays a critical role in regulating cell death processes such as pyroptosis and cuproptosis in CC. Dysregulation of alternative splicing events affecting genes involved in these pathways may contribute to CC development and progression. Elucidating the precise mechanisms underlying the relationship between gene alternative splicing and cell death processes in CC holds promise for identifying novel therapeutic targets and improving patient outcomes. In recent years, some research exploring the influence of alternative splicing to the prognosis of patients bearing cervical cancer were performed [28, 29]. Yet few studies exploit the underlying

correlation between TME phenotype with AS and cellular death modalities. Therefore, exploiting the influence of alternative splicings involved in pyroptosis and cuproptosis to the TME phenotype and survival of patients with CC would be of great benefit not only for the development of targetable immunotherapy drugs and immunotherapy strategies, but also for expanding comprehension to CC.

To address this objective, the present study utilized two publicly available datasets on alternative splicing, focusing on genes associated with cuproptosis and pyroptosis. Various regression methods, including univariate COX, lasso, and multivariate COX, were applied to identify a model comprising five alternative splicing variants involved in pyroptosis and cuproptosis. The analysis involved transcriptome RNA-seq data obtained from cervical cancer patients sourced from the TCGA database. The findings indicated that specific alternative splicing variants related to pyroptosis and cuproptosis played a role in remodeling the tumor microenvironment, thereby influencing immune evasion.

Materials and Methods

Data for Alternative Splicing Model Construction

The survival information and transcriptome data of patients bearing cervical cancer were accessed from the TCGA database (<https://portal.gdc.cancer.gov/>). Eventually, the data of altogether 185 patients after quality control was applied to construct the model (Supplementary Table 1). The corresponding alternative splicing data of these patients was accessed from the website of TCGA SpliceSeq (<https://bioinformatics.mdanderson.org/TCGASpliceSeq/>). Genes involved in pyroptosis and cuproptosis were listed in Supplementary Datasheet 1.

Model Construction

A total of 185 patients were randomly and equally divided into two groups, training and testing cohorts, comprising 93 and 92 patients respectively. The data from the training group was utilized to develop the model, while the data from the testing group was used to evaluate it. Alternative splicings of genes in Supplementary Datasheet 1 were input into the univariate COX regression, setting a p -value less than 0.05 as the filtering condition. Regressions of LASSO and multivariate COX were applied to the alternative splicing variants filtered by the univariate COX, which finally established the model comprising five alternative-splicing variants.

Survival Analysis

The Kaplan–Meier method was used to plot the survival curves, and log-rank was used as the statistical significance test; $p < 0.05$ was considered significant. Patients were scored by the model and labeled with high risk or low risk depending on the comparison to the median score in respective cohorts.

Correlation Analysis of the Alternative Splicing Variants and the Associated Factors

Splicing factors were listed in Supplementary Datasheet 2. In the correlation test, Spearman was chosen as the test method, with a p -value less than 0.05 and the correlation index larger than 0.4 as the filtering threshold.

Correlation Network Construction

The results of correlation between alternative splicing variants and the corresponding splicing factors were constructed with the software Cytoscape.

ESTIMATE

The ESTIMATE (Estimation of STromal and Immune cells in MAlignant Tumor tissues using Expression data) algorithm provided in the R package of estimate was used to assess the composition of tumor microenvironment. ESTIMATE calculates two scores: the StromalScore and the ImmuneScore. The StromalScore reflects the extent of stromal cell infiltration in the tumor tissue, while the ImmuneScore represents the level of immune cell infiltration. These scores are obtained by examining the expression levels of specific genes associated with stromal and immune cell populations. The ESTIMATE algorithm offers a valuable tool for evaluating the tumor microenvironment by estimating the abundance of stromal and immune cells based on gene expression data. Its application facilitates a better understanding of the TME's role in cancer biology and aids in the identification of potential prognostic markers and therapeutic strategies.

CIBERSORT

Loading and running package CIBERSORT with local R software, the gene expression data of patients as the input file. The CIBERSORT (Cell-type Identification By Estimating Relative Subsets Of RNA Transcripts) algorithm is a computational method that plays a crucial role in assessing the tumor microenvironment (TME). It enables the estimation of immune cell populations within complex tissue samples using gene expression data. The CIBERSORT

algorithm provides a valuable tool for evaluating the tumor microenvironment by estimating the relative proportions of immune cell subsets based on gene expression data. Its application facilitates the characterization of immune cell infiltrates and contributes to a deeper understanding of the immune landscape in cancer, leading to potential advancements in diagnosis, prognosis, and immunotherapy.

Differentially Expressed Genes (DEGs)

Patients were scored by the model and labeled with high risk or low risk based on the comparison to the median score. The method of Wilcoxon was used as the difference test for determining the DEGs between the high- and low-risk patients. False discovery rate (FDR) less than 0.1 and \log_2FC larger than one are the significance filtering conditions. The comparison direction was high risk/low risk, which eventually determined 99 DEGs.

Subsets of Enrichment Analysis

GO and KEGG Signaling Pathway Enrichment Analysis

DEGs were input into the GO and KEGG signaling pathway enrichment analyses, “BH” as the adjust method, and only gene set terms and pathways with q -value less than 0.05 were regarded as significant.

Gene Set Enrichment Analysis (GSEA) and Gene Set Variation Analysis (GSVA)

Gene sets of h.all.v2022.1.Hs.symbols.gmt were downloaded from Molecular Signatures Database, and the enriched gene sets with a p -value less than 0.05 and the absolute value larger than one were considered significant. The method of Wilcoxon was used to determine the difference between two groups.

Differential Analysis to the Immune-Associated Gene Sets

The 29 immune-associated gene sets were listed in Supplementary Datasheet 3, which was obtained from the study entitled “Classification of triple-negative breast cancers based on Immunogenomic profiling.” These immune-associated genes, compiled by the authors, are generally applicable and not specific to breast cancer alone. The score of each gene set was calculated by GSVA with the parameter of the method set to “ssgsea,” which was followed by the variation analysis.

Analyses of Variation and Correlation to the Immune-Related Genes

Immune-associated genes were listed in Supplementary Datasheet 4. Wilcoxon and Spearman were adopted to perform the variation and correlation analyses, and a *p*-value less than 0.05 was considered significant.

Tumor Immune Dysfunction and Exclusion (TIDE)

For detailed instructions, please refer to the guidelines provided on the website (<http://tide.dfci.harvard.edu>). Simply put, the gene expression matrix of patients was used as the input file. The Wilcoxon was used to determine the significant difference between patients of high risk and low risk.

Variation Analysis to Drug Sensitivity

By means of R package pRRophetic, the response to drugs of patients was predicted based on the gene expression matrix, followed by the variation analysis with Wilcoxon as the significance testing.

Softwares and Packages

R language: version 4.0.1
primary packages: caret, survival, survminer, glmnet, vioplot, ggplot2, limma, org.Hs.eg.db, clusterProfiler, pRRophetic, ggpvr, corrplot, GSVA, pheatmap, GOplot, enrichplot, estimate, CIBERSORT
Cytoscape: version 3.9.1

Results

Particular Alternative Splicing Variants of Genes Involved in Pyroptosis and Cuproptosis Have the Potential to Serve as Prognostic Markers of Cervical Cancer

It is commonly accepted that distinct splicing variants of the same gene can have completely opposing roles in the development and progression of diseases. Thus, for determining the roles of distinct splicing variants of genes involved in the pyroptosis and cuproptosis in CC, the prognostic model was constructed with the alternative splicing data (Percent Spliced In, PSI) of the genes in the Supplementary Datasheet 1. The prognostic model consisted of five particular alternative splicing variants, CDKN2A|86,000|AP, NFE2L2|56,128|AP, CASP8|56,831|AD, CASP1|18,519|RI, and GSDMD|85,420|AP (Fig. 1 A–C). The risk score of

patients was calculated by the model in the following equation:

$$\text{risk score} = \sum_{i=1}^k \beta_i E_i$$

where the *k* represented the total number of model-comprising members, β denoted the coefficient of the corresponding alternative splicing variant, and *E* indicated the PSI level. Here is the detailed calculation process:

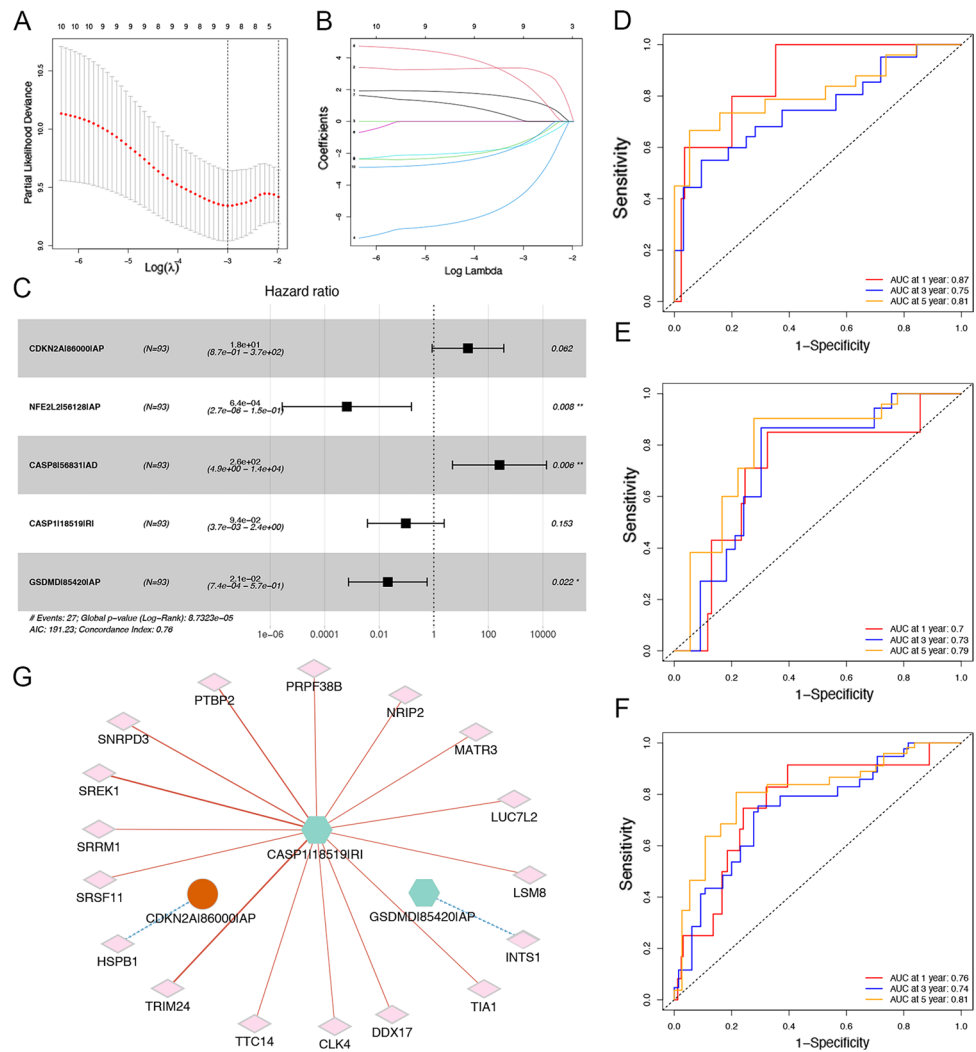
the risk score of the patient = 2.88 * CDKN2A|86000|AP – 7.35
* NFE2L2|56128|AP + 5.55
* CASP8|56831|AD – 2.37
* CASP1|18519|RI – 3.89
* GSDMD|85420|AP.

The receiver operating characteristic (ROC) curve analysis was conducted to evaluate the performance of the model separately across different groups including training, testing, and all patients (Fig. 1D–F). The analysis results of the ROC curve demonstrated that the model exhibits relatively good performance across different subgroups. It showed good predictive ability for 1-year, 3-year, and 5-year prognoses. To identify the factors underlying the model-constituting alternative splicing variants, correlation analysis was performed. The findings showed that three splicing variants were found to be correlated with corresponding alternative splicing factors. Among them, CDKN2A|86,000|AP and GSDMD|85,420|AP had only one splicing-related factor each, namely HSPB1 and INTS1, respectively (Fig. 1G). In order to thoroughly assess how effective the model is at predicting the prognosis of CC patients, we conducted overall and conditional survival analyses. The results showed that patients who were deemed to have a higher risk by the model had significantly worse prognoses than those who were classified as low risk, regardless of which group they were in (Fig. 2). The aforementioned results convincingly indicate that the five alternative splicing variants of the model possess the potential to serve as robust prognostic indicators for patients diagnosed with CC.

The Model-Associated Alternative Splicing Variants Are Associated with Distinct Immune Compositions in Patients with CC

Given the close association between CC and HPV infection, the composition of TME plays a pivotal role in the initiation and progression of CC. In light of the discovery of novel forms of cell death, such as pyroptosis and ferroptosis, it becomes crucial to further investigate and pay attention to their potential association with alterations in the components of TME. The ESTIMATE algorithm enables the estimation of immune and

Fig. 1 Construction of the alternative splicing prognostic model and correlation analysis to the model-comprising variants and the associated factors. **A, B** LASSO coefficient profiles and determination of the tuning parameter (lambda) in the LASSO model established on the partial likelihood deviance with tenfold cross-validation. **C** Forest plot of multivariate Cox regression. **D–F** Evaluation of the model performance separately across training, testing, and all patient groups. **G** Correlation analysis of model-constituting splicing variants and the associated alternative splicing factors. The two hexagons in green color indicated the alternative splicing variants belonging to the gene set of pyroptosis, playing protective roles in the hazard model; the circle in red color denoted the alternative splicing variant grouped in the cuproptosis-associated gene set, being a harmful hazard factor in the model; the diamond shape with pink color signified the alternative splicing factors associated with the model-constituting variants; solid red lines linking the variants and associated splicing factors denoted positive correlation, and the green dashed lines depicted the negative correlation



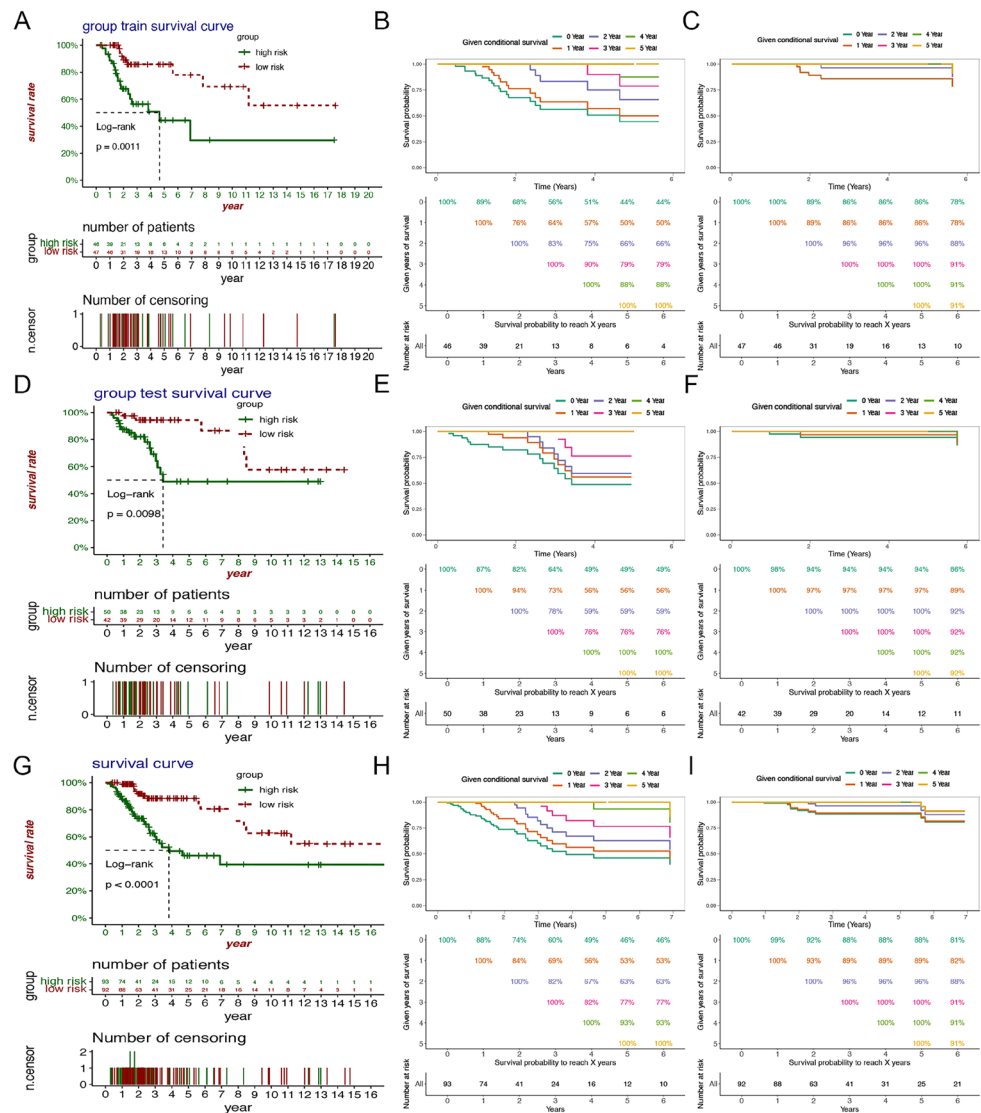
stromal components within TME, facilitating the evaluation of compositional differences in TME between patients classified as high or low risk by the model. The results demonstrated a notable increase in the immune composition of the tumor microenvironment (TME) among patients with lower risk, in contrast to patients with higher risk, where the immune composition was comparatively lower. Conversely, these differences were reflected in the tumorous content (Fig. 3). The results indicated a significant correlation between the expression level of specific alternative splicing variants of the five genes involved in pyroptosis and cuproptosis and the immune composition of the TME in patients with CC.

The Alternative Splicing Variants that Constitute the Model Were Found to be Associated with the Composition of Tumor-Infiltrating Immune Cells (TICs)

Based on the preceding results, it was observed that the splicing variants exhibited a correlation with the immune

composition of the TME in CC. These findings highlight the need for further exploration into the characterization of tumor-infiltrating immune cells (TICs) in patients stratified by varying degrees of risk predicted by the model. Therefore, the CIBERSORT algorithm was applied to quantify the abundance of tumor-infiltrating immune cells (TICs), thereby elucidating the correlation between splicing variants and TICs in patients with CC. The results revealed distinct patterns of TIC infiltration within the microenvironment across different patient groups, involving a panel of seven immune cell types, namely, B cells naive, CD8+ T cells, gamma delta T cells, M0 macrophages, resting dendritic cells, resting mast cells, and activated mast cells (Fig. 4A). Among these immune cell types, except for M0 macrophages and activated mast cells, the proportions of the remaining cell types showed a significant decrease in the high-risk group compared to the low-risk group. To further investigate the interplay between different TICs and their association with the risk score calculated by the model, a correlation analysis was performed. The findings

Fig. 2 Overall and conditional survival analyses. **A–C** Overall survival analyses with entire patients in the training group, conditional survival analyses of high- and low-risk patients in the training group. **D–F** Overall survival analysis to the entire patients in the testing group, conditional survival analyses of high- and low-risk patients in the testing cohort. **G–I** Overall survival curves depicting the entire patients, conditional survival analyses of high- and low-risk patients in all patients cohort

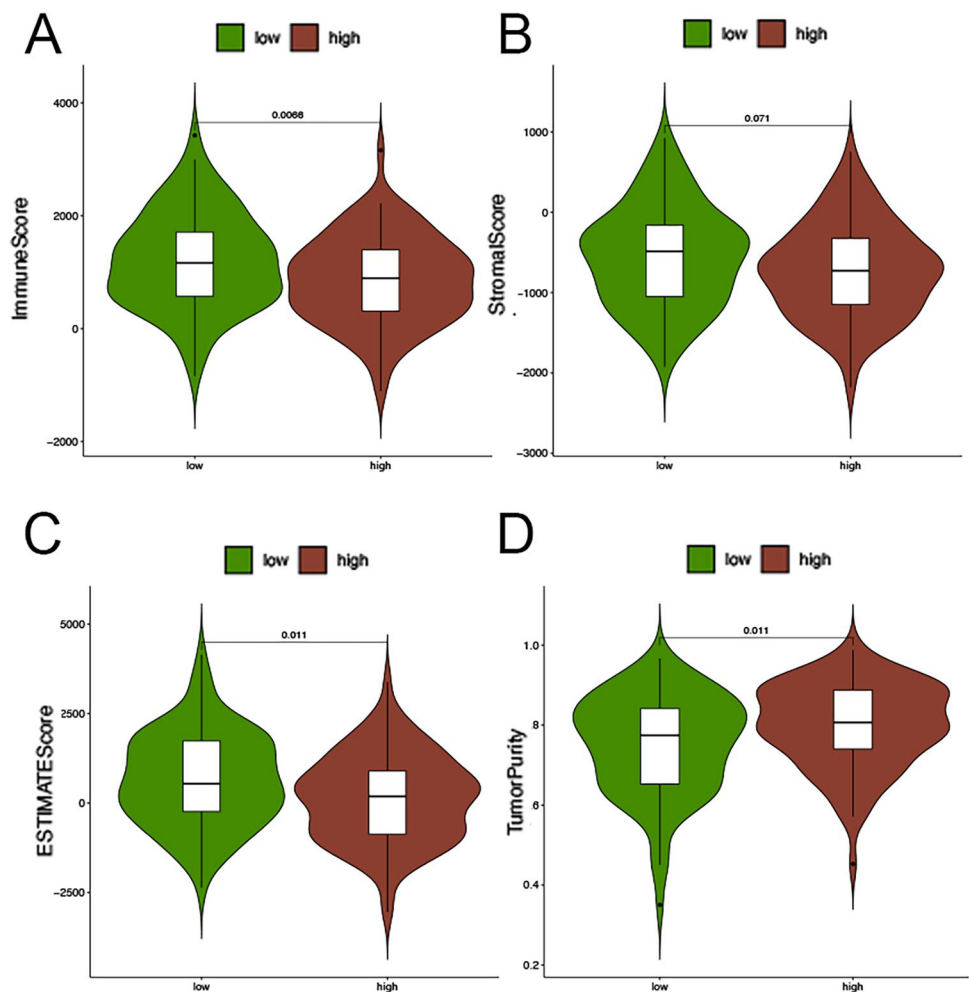


revealed significant correlations between the risk score and six immune cell types, namely CD8 + T cells, follicular helper T cells, M0 macrophages, resting dendritic cells, resting mast cells, and activated mast cells (Fig. 4B). To obtain a more concise overview, a separate analysis was conducted focusing on the six significant immune cell types. Subsequently, another correlation analysis was performed. Among these cell types, M0 macrophages and activated mast cells exhibited a positive correlation with the risk score of patients. In contrast, CD8 + T cells, follicular helper T cells, resting dendritic cells, and resting mast cells displayed a negative correlation with the risk score (Fig. 4C and Supplementary Fig. 1).

The Specific Alternative Splicing Events in Pyroptosis-Associated and Cuproptosis-Related Genes Contribute to the Phenotypic Remodeling of the TME in Patients with Cervical Tumors

The phenotype of the TME plays a significant role in indicating the status and progression of tumors, including metastasis, proliferation, regression, and drug resistance. To investigate the impact of specific variants resulting from alternative splicing, particularly those associated with pyroptosis or cuproptosis, on the TME phenotype in CC, a series of enrichment analyses were conducted. Initially, a set of differentially expressed genes (DEGs) was obtained,

Fig. 3 ESTIMATE algorithm to calculate the ratio of immune composition, stromal composition, and tumor purity. **A–D** ImmuneScore, indicating the proportion of immune-associated components; StromalScore, reflecting the amount of stromal-related composition; ESTIMATEScore, representing the comprehensive proportion of the immune- and stromal-associated composition; TumorPurity, showing the relative amount of tumors



comprising a total of 99 genes, with 38 up-regulated and 61 down-regulated in high-risk patients compared to low-risk patients (Fig. 5A). Following that, Gene Ontology (GO) and Kyoto Encyclopedia of Genes and Genomes (KEGG) pathway enrichment analyses were performed using the set of 99 DEGs. The GO analysis encompassed three main categories: biological process, cellular component, and molecular function. The results revealed notable enrichments in the molecular function (MF) category, particularly in stimulus-related signaling pathways such as cytokine receptor binding, chemokine receptor binding, cytokine activity, chemokine activity, G protein-coupled receptor binding, CXCR chemokine receptor binding, signaling receptor activator activity, and receptor-ligand activity, predominantly observed in the high-risk patient group. In contrast, the low-risk patient group exhibited significant enrichments in enzymatic reactions, metabolic activities, and immune-related functions, including oxidoreductase activity, acting on single donors with incorporation of molecular oxygen, antigen binding, and endopeptidase activity, among others (Fig. 5B). These findings highlight the divergent functional

profiles between high-risk and low-risk patients, shedding light on the underlying biological processes associated with the distinct phenotypes of the TME in cervical cancer. Similar findings were observed in the cellular component category, revealing enrichments of immune-related activities in the low-risk patient group, for example, the T-cell receptor complex. In contrast, the gene set associated with the tertiary granule lumen showed significant enrichment in the high-risk patient group, suggesting an immunosuppressive status. This observation is supported by the fact that compared to secondary granules, tertiary granules have a lower concentration of antimicrobial substances and are more readily exocytosed. Thus, tertiary granules serve as a primary reservoir for extracellular matrix-degrading enzymes and membrane receptors that are crucial for cellular migration (Fig. 5B). These findings provide insights into the distinct cellular components and their functional implications in the TME of cervical cancer patients with varying risk profiles. Differences in the cellular activity status of the tumor microenvironment (TME) in patients with varying risk profiles were evident through the enriched terms in the biological

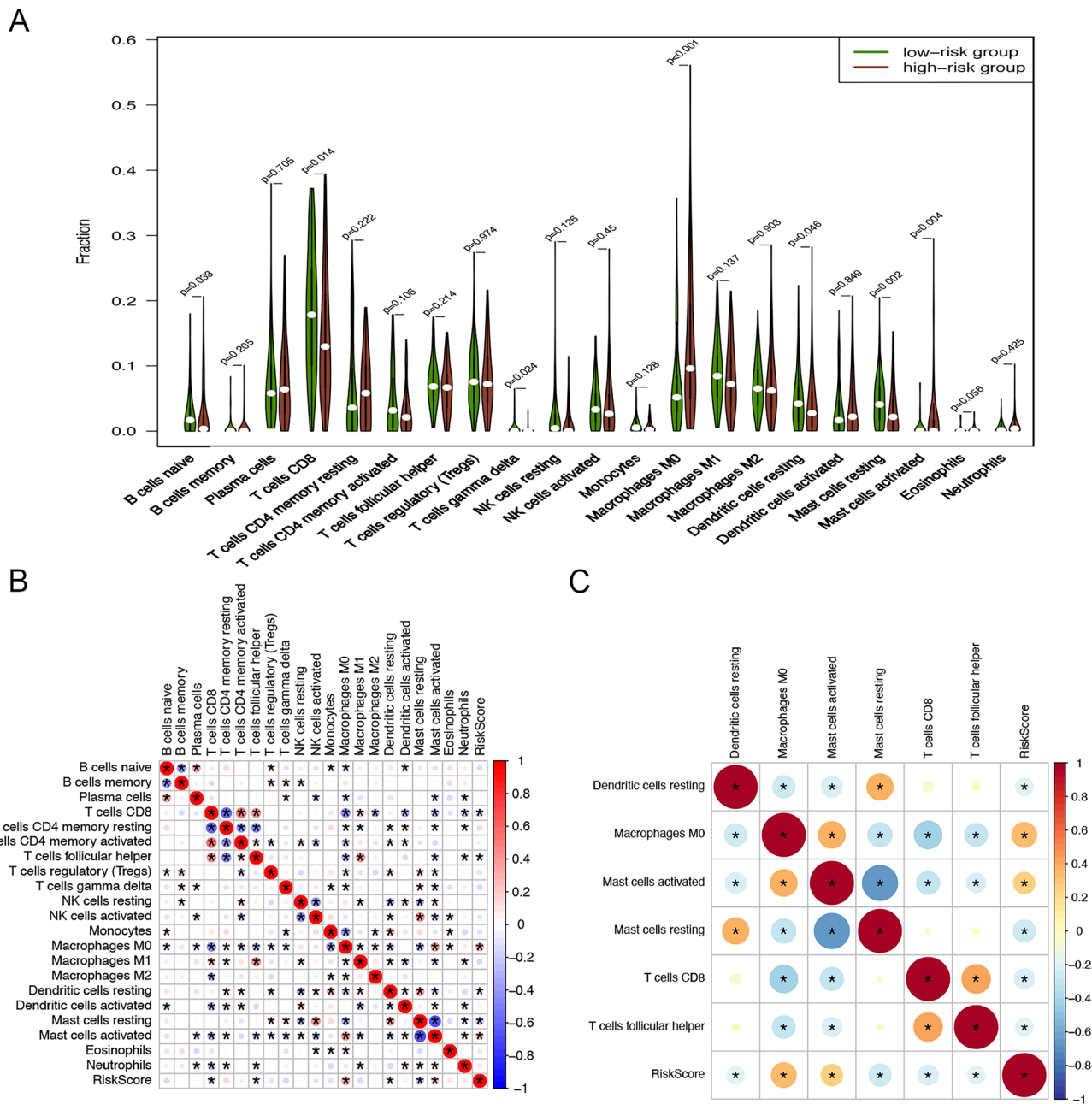


Fig. 4 CIBERSORT algorithm to evaluate the composition of tumor-infiltrating immune cells (TICs). **A** CIBERSORT algorithm to calculate the relative amount of TICs. **B** Correlation analysis of TICs with the risk score calculated by the prognostic model. The symbol

of asterisk denoted the significant relationship between two factors, and the color symbolized the strength of the correlation. **C** Detailed display of correlation between six significant kinds of TICs and the risk score

process category. Specifically, high-risk patients showed enrichments in terms related to cellular migration and adhesion (Fig. 5B). The GO enrichment analysis indicated that high-risk patients exhibited a tumor-promoting phenotype characterized by enhanced cellular migration, as well as dynamic cytokine and chemokine activities. In contrast, the TME of low-risk patients exhibited an immune-focused phenotype, with significant enrichments in immune activities.

Similarly, the enrichment analysis of KEGG signaling pathways yielded comparable results. Specifically, three signaling pathways, namely antigen processing and presentation, neuroactive ligand-receptor interaction, and natural killer cell-mediated cytotoxicity, were significantly enriched in the TME of low-risk patients (Fig. 5C). In contrast, the enrichment analysis revealed that high-risk patients exhibited significant enrichments in several signaling pathways

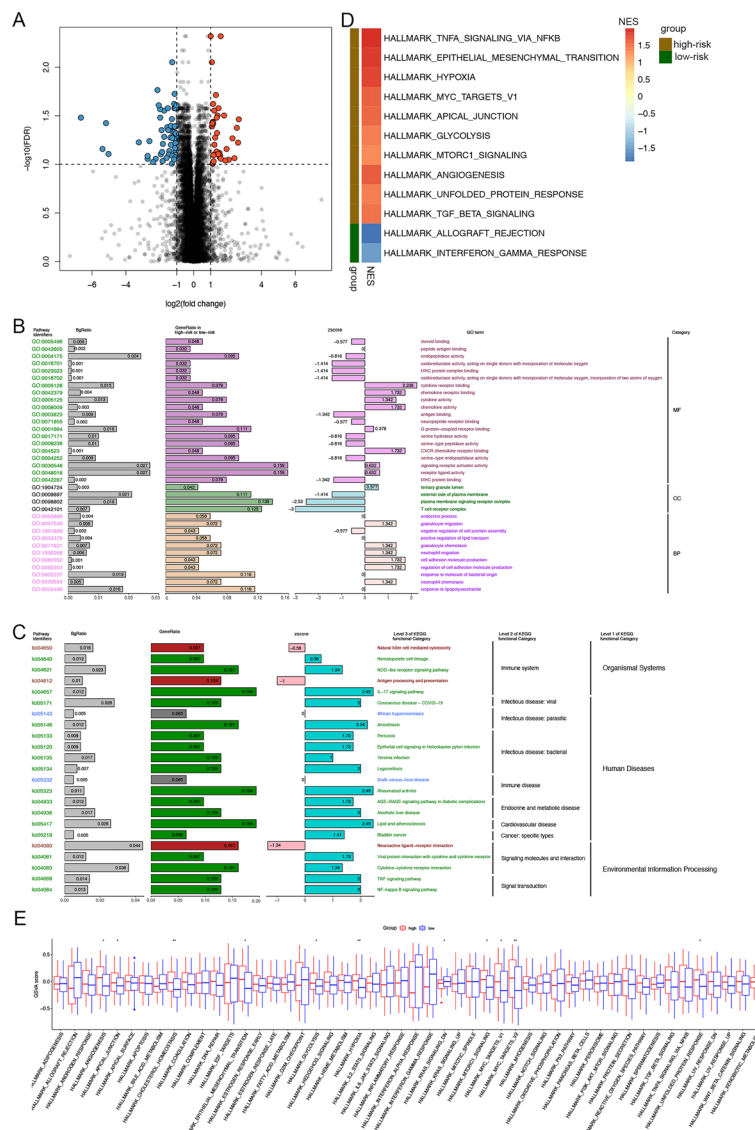


Fig. 5 Generation of differentially expressed genes (DEGs) and analyses of enrichment and variation. **A** DEGs with FDR less than 0.1 and $\log_2\text{FC}$ larger than 1 were considered significant, and a total of 38 upregulated and 61 downregulated DEGs were established in high-risk patients compared to the low-risk. **B** GO enrichment analysis with the DEGs, molecular function (MF), cellular component (CC), and biological process (BP) three categories were enriched respectively. Z-score larger than zero suggested the gene sets were enriched in high-risk patients, and on the contrary, less than zero indicated enriched by the low-risk patients. **C** KEGG signaling path-

way enrichment analysis with DEGs. Z-score larger than zero denoted the signaling pathways were enriched in high-risk patients, and conversely, less than zero signified enriched by the low-risk patients. The hierarchy structure of signaling pathways was exhibited by three levels. **D** Gene Set Enrichment Analysis (GSEA) with the HALLMARK gene sets downloaded from Molecular Signatures Database; NES, normalized enrichment score. **E** Gene Set Variation Analysis (GSVA) with the HALLMARK gene sets accessed from Molecular Signatures Database; one symbol of asterisk denoted the p -value less than 0.05, two asterisks, less than 0.01, Wilcox as the testing method

associated with disease-related processes and signal transduction. These pathways included bladder cancer, pertussis, alcoholic liver disease, NF-kappa B signaling pathway, and NOD-like receptor signaling pathway (Fig. 5C).

Based on the enrichment analyses conducted, it is evident that the TME phenotypes of high-risk and low-risk patients exhibit significant differences. High-risk patients exhibited an active cellular metabolism, extensive cellular

interactions, and enhanced cellular motility, indicative of a tumor-promoting phenotype. Conversely, low-risk patients displayed an immune-preferential phenotype characterized by notable immune-related activities. These observations emphasize the importance of considering the distinct TME phenotypes associated with varying risk profiles in cervical cancer patients. To comprehensively investigate the status of the microenvironment, we conducted Gene Set Enrichment

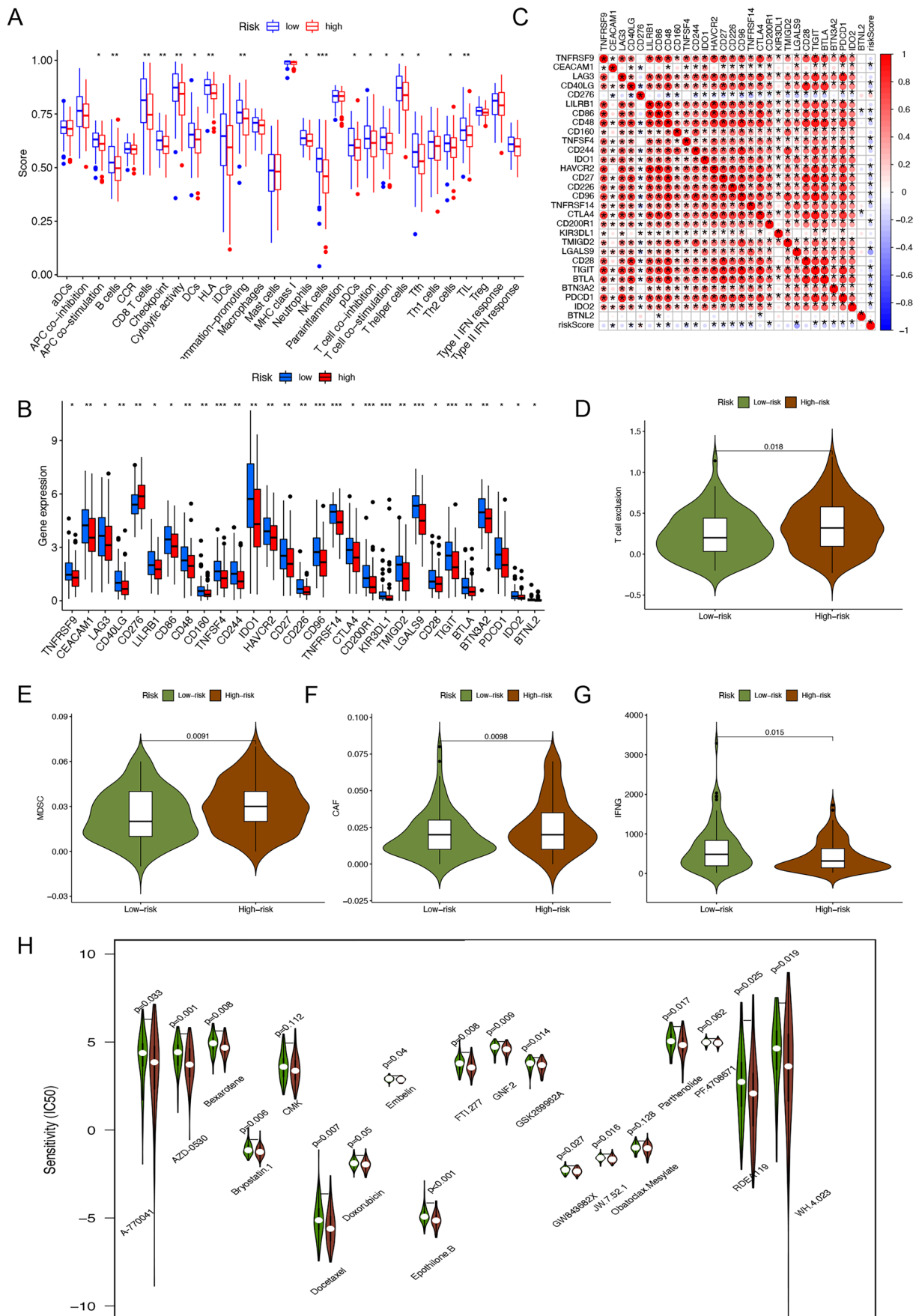


Fig. 6 Immune-associated variation and correlation analyses. **A** The immune-associated gene sets were scored by GSVA, followed by variation analysis. One symbol of asterisk denoted a p -value less than 0.05, two representing 0.01, and three signifying 0.001. **B** Differential analysis of immune checkpoint-related genes, one asterisk symbol denoting a p -value less than 0.05, two representing 0.01, three indicating 0.001, and Wilcox as the significance testing method. **C** Correlation analysis of immune checkpoint-associated genes, the asterisk signifying a p -value less than 0.05, and the color filled in the circle represented the strength of the correlation between two factors. **D–G** Analysis of Tumor Immune Dysfunction and Exclusion (TIDE). Variation analyses regarding aspects of T-cell exclusion, myeloid-derived suppressor cells (MDSCs), cancer-associated fibroblasts (CAFs), and interferon-gamma (IFNG). **H** Variation analysis of the predicted drug response

Analysis (GSEA) using HALLMARK gene sets from the Molecular Signatures Database. Strikingly, we observed significant enrichments of metabolism-related gene sets in the high-risk group, including EPITHELIAL_MESENCHYMAL_TRANSITION, GLYCOLYSIS, ANGIOGENESIS, MYC_TARGETS_V1, and APICAL_JUNCTION, indicating an active TME that promotes tumor growth and progression (Fig. 5D). In contrast, the low-risk patients exhibited enrichments in two gene sets, ALLOGRAFT_REJECTION and INTERFERON_GAMMA_RESPONSE, which are indicative of an immune-related response. The results further support the immune-preferring status of the TME in the low-risk group (Fig. 5D). The findings align with previous studies demonstrating that cervical cancer (CC) employs energy-efficient metabolic pathways, such as hypoxia and glycolysis, to promote rapid proliferation, giving it a competitive advantage over adjacent normal tissue cells. To further elucidate the divergent phenotypic characteristics of the TME between high- and low-risk patients, Gene Set Variation Analysis (GSVA) was performed, employing HALLMARK gene sets as the target. Consistent with the previously reported GSEA results, significant enrichment of tumor-favoring gene sets was observed in high-risk patients, including HALLMARK_ANGIOGENESIS, HALLMARK_APICAL_JUNCTION, HALLMARK_EPITHELIAL_MESENCHYMAL_TRANSITION, and HALLMARK_GLYCOLYSIS, HALLMARK_HYPOXIA (Fig. 5E).

Specific Alternative Splicing Events in Pyroptosis and Cuproptosis Are Linked to Immune Evasion and Chemotherapy Sensitivity

Based on the preceding series of enrichment analyses, it can be safely concluded that a remodeling occurred in the phenotype of the TME, contributed by the variants involved in two kinds of cellular death modalities, pyroptosis and cuproptosis, generated by particular alternative splicings. Collectively, this observation represents a plasticity in the TME phenotype, characterized by a transition between a

tumor-favoring phenotype and an immune-preferring phenotype, which is comprehensively influenced by alternative splicing variants. Although some patients have shown positive responses to immunotherapy, a significant proportion of tumor patients fail to respond to immune-based treatments. This lack of response may be closely associated with the immune phenotype of the TME, specifically the immune-related characteristics of the TME. To further investigate the impact of alternative splicing variants on the immune phenotype of the TME, Gene Set Variation Analysis (GSVA) was conducted, targeting 29 gene sets that are relevant to the immune system. These gene sets encompass a wide range of immune cells, immune-related signaling pathways, and immune-associated functions. The analysis revealed notable differences in various immune-related functions and cell types between high-risk and low-risk patients, including B cells, antigen-presenting cell (APC) co-stimulation, CD8+ T cells, natural killer (NK) cells, immune checkpoint pathways, dendritic cells (DCs), tumor-infiltrating lymphocytes (TILs), and T helper cells (Fig. 6A). High-risk patients exhibited weaker expression levels in all of the immune-associated gene sets analyzed, compared to low-risk patients. These findings are consistent with the earlier observation that patients with lower risk scores tend to have an immune-preferring phenotype in the TME, and to some extent, this may explain why low-risk patients have better prognoses than high-risk patients who adopt a tumor-favoring phenotype in the TME. Additionally, an analysis of the expression of immune-related genes was conducted, which revealed that high-risk patients had significantly lower expression levels of these genes than low-risk patients (Fig. 6B). Correlation analysis supported this observation, as the risk score was found to be negatively correlated with the expression of immune-related genes, with the exception of CD276 (Fig. 6C and Supplementary Fig. 2). To further investigate the influence of different TME phenotypes on immune evasion and to evaluate the underlying mechanism used by tumors to evade immune surveillance, we utilized the web platform TIDE (<http://tide.dfci.harvard.edu>) to calculate patient scores with respect to T-cell exclusion and associated cells, such as myeloid-derived suppressor cells (MDSCs) and cancer-associated fibroblasts (CAFs). Our results demonstrated that, except for interferon-gamma (IFNG), high-risk patients had higher scores for T-cell exclusion, MDSCs, and CAFs compared to low-risk patients. These findings further support our earlier conclusion that the TME in high-risk patients exhibits a tumor-favoring phenotype that is immune-suppressive, characterized by T-cell exclusion, and that this may also correlate with MDSCs and CAFs (Fig. 6D, E, F, and G). Since chemotherapy remains a major treatment option in clinical practice, we explored the influence of TME phenotype remodeling on tumor sensitivity to chemotherapy drugs. Using the R package, we predicted the

sensitivities of patients to various chemotherapy drugs. The results clearly showed that patients with higher risk scores were more vulnerable to many chemotherapy drugs, with lower IC50 values compared to low-risk patients (Fig. 6H). These findings highlight the significance of TME phenotype in clinical treatment with chemotherapy drugs and provide clinicians with additional treatment options.

Discussion

The results of this study suggested that the occurrence of particular alternative splicing events in genes involved in pyroptosis and cuproptosis was implicated in the phenotypic remodeling of TME. The role of pyroptosis- and cuproptosis-associated alternative splicing in remodeling the TME of cervical cancer was explored from three aspects in this study. First, TME composition analyses and a series of enrichment analyses revealed distinct TME characteristics between the high- and low-risk groups, particularly the tumor-favoring phenotype in high-risk patients. Second, differences in immune-related gene sets and immune-related genes between the two groups, as well as their risk associations, indicated differential immune phenotypes of the TME. Third, differences in immune escape and drug sensitivity between the two groups further suggested distinct immune phenotypes of the TME, with a TME phenotype in high-risk patients promoting immune evasion of tumor cells.

The results that the expressions of many immune-related genes were significantly higher in the low-risk group compared to the high-risk group provide important insights into the immune landscape and potential prognostic implications in cervical cancer. One possible explanation for the higher expression of immune-related genes in the low-risk group compared to the high-risk group of cervical cancer patients is the presence of an active and responsive immune system in the low-risk group. It is known that the immune system plays a crucial role in recognizing and eliminating cancer cells. In the context of cervical cancer, a robust immune response is associated with improved prognosis and better treatment outcomes. The higher expression of immune-related genes in the low-risk group could reflect enhanced immune cell activation and infiltration within the tumor microenvironment. This immune activation may be driven by the presence of specific immune cell populations, such as B cells naive, CD8+ T cells, gamma delta T cells, resting dendritic cells, and resting mast cells, which were found to be significantly enriched in the tumor tissue of the low-risk group. These immune cells are known to play important roles in orchestrating anti-tumor immune responses, including the recognition and killing of cancer cells. Furthermore, the enrichment analysis results indicated that the low-risk group exhibited a significant enrichment in immune-related activities. This enrichment may signify the activation of pathways involved

in immune surveillance, antigen presentation, T-cell activation, and cytokine signaling, among others. These processes collectively contribute to an effective anti-tumor immune response. It is important to note that the higher expression of immune-related genes in the low-risk group does not necessarily indicate that these genes are promoting tumor development. Instead, it suggests that the immune system in the low-risk group is actively engaged in recognizing and responding to the tumor, potentially leading to better control of tumor growth and improved patient outcomes. In contrast, the high-risk group exhibited a lower expression of immune-related genes, which may indicate a compromised or suppressed immune response. This impaired immune activity could contribute to a less effective tumor immune surveillance and clearance, allowing the tumor to evade immune recognition and potentially progress more aggressively. In summary, the higher expression of immune-related genes in the low-risk group compared to the high-risk group of cervical cancer patients suggests an activated and responsive immune system in the low-risk group. This enhanced immune response, characterized by specific immune cell populations and immune-related pathway enrichment, may contribute to better prognosis and improved patient outcomes by effectively targeting and eliminating cancer cells.

In this study, it was explicitly stated that the stratification of patients into high-risk and low-risk groups was based on a model established using alternative splicing data related to pyroptosis and cuproptosis. The distinct characteristics observed in the TME of the two risk groups, as assessed by a set of enrichment analyses, and the algorithms of ESTIMATE and CIBERSORT, provided evidence supporting the role of pyroptosis and cuproptosis in remodeling the TME in cervical cancer. The higher ImmuneScore observed in the low-risk group suggests an increased presence of immune cells and heightened immune activity within their TME. This finding aligns with previous studies demonstrating that pyroptosis can trigger the release of pro-inflammatory cytokines, leading to an enhanced immune response against tumor cells. Additionally, the enrichment of immune cell populations, such as B cells naive, CD8+ T cells, gamma delta T cells, resting dendritic cells, and resting mast cells, in the tumor tissue of the low-risk group further supports the notion that the alternative splicing variants involved in pyroptosis and cuproptosis play a role in shaping the immune landscape of the TME. Furthermore, the enrichment analysis results revealed that the low-risk group exhibited enrichment in immune-related activities, while the high-risk group showed enrichment in processes associated with hypoxia, glycolysis, and epithelial-mesenchymal transition (EMT). These observations align with existing knowledge that pyroptosis-induced release of pro-inflammatory cytokines can promote an immune-active TME and cuproptosis-associated alterations in cellular copper levels may affect metabolic reprogramming and EMT, contributing to a more aggressive tumor phenotype.

Therefore, based on the significant differences observed in the TME phenotype of the high-risk and low-risk groups, which were stratified using a model built on alternative splicing variants involved in pyroptosis and cuproptosis, these findings in this study suggested that particular alternative splicing variants involved in pyroptosis and cuproptosis contribute to the remodeling of the TME in cervical cancer by modulating immune responses and metabolic pathways. These findings highlight the importance of considering the impact of these cell death pathways on the TME phenotype and provide insights into the potential mechanisms by which pyroptosis and cuproptosis influence tumor progression and patient prognosis.

Supplementary Information The online version contains supplementary material available at <https://doi.org/10.1007/s43032-023-01284-y>.

Data Availability The data used in this study could be accessed from freely public-accessible database including databases of TCGA (<https://portal.gdc.cancer.gov/>), Molecular Signatures (<https://www.gsea-msigdb.org/gsea/msigdb/>), and TCGA SpliceSeq (<https://bioinformatics.mdanderson.org/TCGASpliceSeq/>).

Code Availability Raw data and codes are available on request.

Declarations

Ethics Approval The databases of TCGA and websites used in this work are open free to the public, the data of patients deposited in TCGA have obtained ethical approval, and this study is based on open-source data, so there are no ethical issues and other conflicts of interest.

Consent to Participate Not applicable.

Consent for Publication Not applicable.

Competing Interests The authors declare no competing interests.

References

1. Fernandes A, et al. Human papillomavirus-independent cervical cancer. *Int J Gynecol Cancer*. 2022;32(1):1–7.
2. Ferrall L, et al. Cervical cancer immunotherapy: facts and hopes. *Clin Cancer Res*. 2021;27(18):4953–73.
3. Ge EJ, et al. Connecting copper and cancer: from transition metal signalling to metalloplasia. *Nat Rev Cancer*. 2022;22(2):102–13.
4. Song Y, et al. HPV E7 inhibits cell pyroptosis by promoting TRIM21-mediated degradation and ubiquitination of the IFI16 inflammasome. *Int J Biol Sci*. 2020;16(15):2924–37.
5. Li L, et al. Pyroptosis, a new bridge to tumor immunity. *Cancer Sci*. 2021;112(10):3979–94.
6. Lee C, et al. Inflammasome as a promising therapeutic target for cancer. *Life Sci*. 2019;231:116593.
7. Tong X, et al. Targeting cell death pathways for cancer therapy: recent developments in necroptosis, pyroptosis, ferroptosis, and cuproptosis research. *J Hematol Oncol*. 2022;15(1):174.
8. Zhou C, et al. Identification of pyroptosis-related signature for cervical cancer predicting prognosis. *Aging (Albany NY)*. 2021;13(22):24795–814.

9. Sharma BR, Kanneganti TD. NLRP3 inflammasome in cancer and metabolic diseases. *Nat Immunol*. 2021;22(5):550–9.
10. Hamarshah S, Zeiser R. NLRP3 inflammasome activation in cancer: a double-edged sword. *Front Immunol*. 2020;11:1444.
11. Dey Sarkar R, Sinha S, Biswas N. Manipulation of inflammasome: a promising approach towards immunotherapy of lung cancer. *Int Rev Immunol*. 2021;40(3):171–82.
12. Yu SY, Li XL. Pyroptosis and inflammasomes in obstetrical and gynecological diseases. *Gynecol Endocrinol*. 2021;37(5):385–91.
13. Huang Y, Li R, Yang Y. Role of pyroptosis in gynecological oncology and its therapeutic regulation. *Biomolecules*. 2022;12(7):924.
14. Lei L, Tan L, Sui L. A novel cuproptosis-related gene signature for predicting prognosis in cervical cancer. *Front Genet*. 2022;13:957744.
15. Chen SJ, et al. Mechanistic basis of a combination D-penicillamine and platinum drugs synergistically inhibits tumor growth in oxaliplatin-resistant human cervical cancer cells in vitro and in vivo. *Biochem Pharmacol*. 2015;95(1):28–37.
16. Lelièvre P, et al. The multifaceted roles of copper in cancer: a trace metal element with dysregulated metabolism, but also a target or a bullet for therapy. *Cancers (Basel)*. 2020;12(12):3594.
17. Bandmann O, Weiss KH, Kaler SG. Wilson's disease and other neurological copper disorders. *Lancet Neurol*. 2015;14(1):103–13.
18. Zhang M, Shi M, Zhao Y. Association between serum copper levels and cervical cancer risk: a meta-analysis. *Biosci Rep*. 2018;38(4):BSR20180161.
19. Tsvetkov P, et al. Copper induces cell death by targeting lipoylated TCA cycle proteins. *Science*. 2022;375(6586):1254–61.
20. Zhang Z, et al. Cuproptosis-related risk score predicts prognosis and characterizes the tumor microenvironment in hepatocellular carcinoma. *Front Immunol*. 2022;13:925618.
21. Bao JH, et al. Identification of a novel cuproptosis-related gene signature and integrative analyses in patients with lower-grade gliomas. *Front Immunol*. 2022;13:933973.
22. Xu S, et al. Cuproptosis-associated lncRNA establishes new prognostic profile and predicts immunotherapy response in clear cell renal cell carcinoma. *Front Genet*. 2022;13:938259.
23. Voli F, et al. Intratumoral copper modulates PD-L1 expression and influences tumor immune evasion. *Cancer Res*. 2020;80(19):4129–44.
24. Wang ET, et al. Alternative isoform regulation in human tissue transcriptomes. *Nature*. 2008;456(7221):470–6.
25. Keren H, Lev-Maor G, Ast G. Alternative splicing and evolution: diversification, exon definition and function. *Nat Rev Genet*. 2010;11(5):345–55.
26. Oltra SS, et al. Distinct GSDMB protein isoforms and protease cleavage processes differentially control pyroptotic cell death and mitochondrial damage in cancer cells. *Cell Death Differ*. 2023;30(5):1366–81.
27. Gupta A, Lutsenko S. Human copper transporters: mechanism, role in human diseases and therapeutic potential. *Future Med Chem*. 2009;1(6):1125–42.
28. Ouyang D, et al. Comprehensive analysis of prognostic alternative splicing signature in cervical cancer. *Cancer Cell Int*. 2020;20:221.
29. Shao XY, et al. Prognostic value and potential role of alternative mRNA splicing events in cervical cancer. *Front Genet*. 2020;11:726.

Publisher's Note Springer Nature remains neutral with regard to jurisdictional claims in published maps and institutional affiliations.

Springer Nature or its licensor (e.g. a society or other partner) holds exclusive rights to this article under a publishing agreement with the author(s) or other rightsholder(s); author self-archiving of the accepted manuscript version of this article is solely governed by the terms of such publishing agreement and applicable law.